

NON-LINEAR FINITE ELEMENT ANALYSIS OF STEEL FIBRE REINFORCED BEAMS WITH CONVENTIONAL REINFORCEMENT

David Fall^{*}, Rasmus Rempling^{*}, Anette Jansson^{*}, Karin Lundgren^{*} and Kent Gylltoft^{*}

^{*} Dep. of Civil and Environmental Engineering, Div. of Struct. Eng., Chalmers University of Technology
Sven Hultins Gata 8, 412 96 Gothenburg, Sweden
e-mail: david.fall@chalmers.se, web page: www.chalmers.se

Keywords: Steel fibre reinforced concrete, reinforced concrete beams, non-linear FE modelling, fib Model Code 2010

Summary: *The purpose of this study has been to investigate the behavior of elements reinforced with both conventional steel reinforcement and steel fibres in order to support future applications of such composites. Three beams of varying fibre content were tested in four-point bending. The results were then compared with results from nonlinear FE-analyses and the calculation method suggested in fib Model Code 2010. The beams were a part of a larger experimental programme where relevant properties were investigated in uniaxial tension tests and pull-out tests. The FE-modeling was performed using a two dimensional plane stress model. General agreement between experiments and the FE-analyses was obtained with regard to load-displacement behavior. The crack patterns from the FE-analysis and experiments agreed in general, although the crack patterns in the analysis were more distributed close to the reinforcement. Crack localization was enhanced by modifying the bond-slip behavior to include the bond loss at yielding. Calculations in accordance with fib Model Code 2010 yield conservative results in comparison with both experiments and FE-analysis.*

1 INTRODUCTION

Although, the use of steel fibre reinforcement (SFRC) has increased during the last two decades, it could also be claimed that the anticipated development has been hindered by the lack of design regulations. Several researchers have studied laboratory scale tests with the purpose to determine material properties for SFRC. Approaches of determining the tensile behaviour of SFRC have been discussed in numerous articles. Methods based on uniaxial testing and beam bending have been suggested [1, 2]. In addition to these methods, a wedge-splitting procedure was proposed [3]. Larger scale beams have been studied [4, 5]; however, there still is a lack of studies of SFRC, relevant to practice, performed with well-defined material parameters. The current study was performed to contribute to the field of SFRC modelling. Establishing a broad knowledge of the structural behavior and design methods of SFRC is important in order to enable a wider usage of the technology. By combining experimental work and non-linear finite element analysis and comparing these with results from calculations in accordance with fib Model Code 2010 (MC 2010), this paper evaluates the structural engineering approaches to SFRC.

2 EXPERIMENTAL PROGRAMME

The experimental programme comprised uniaxial testing, pull-out tests, reinforcement tension tests and four-point bending test of beams. Although the main focus of this paper is the concrete beams, the other experiments are described here in concentrated form. Full descriptions of the pull-out tests and uniaxial tests are provided by Jansson et al. [6, 7].

2.1 Four-point bending

Three SFRC beams of fibre content 0.0, 0.25 and 0.5% (percent by volume) were tested in deformation controlled four-point bending. The beams were simply supported and spanned 1800 mm, with shear spans of 600 mm, see Figure 1. Support settlements and deflections were recorded. Deflections were measured at mid-span and at the loading positions. At all measuring points, two displacement transducers were used. Identical test set-ups have previously been used [8, 9]. Three reinforcement bars were used as bending reinforcement in each beam: $\varnothing 8$ in the beams of fibre content 0.0 and 0.5% and $\varnothing 6$ in the beam of fibre content 0.25%. Steel quality was B500BT (Swedish quality). Shear reinforcement (stirrups) was included over the supports. Fibre content, reinforcement configurations and tested strengths for all beams are presented in Table 1.

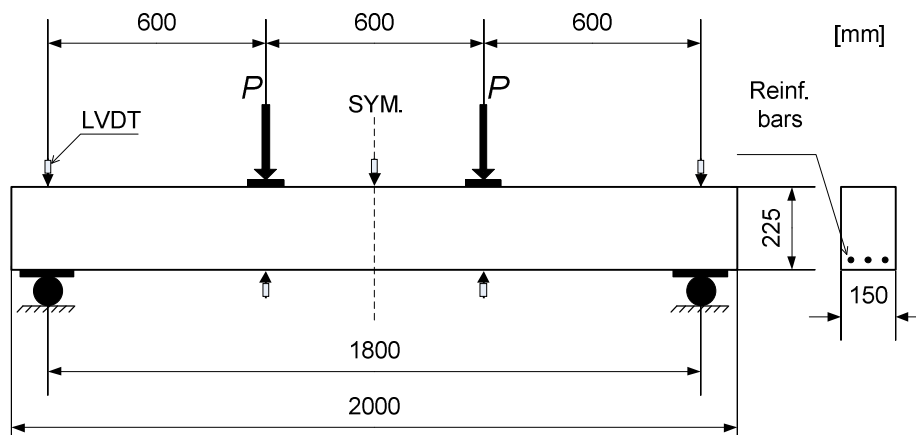


Figure 1: Experimental set-up

Table 1: Test beam configurations

Beam No.	I	II	III
V_f , nominal	-	0.25%	0.50%
V_f , actual (mean value from wash-out)	-	0.18%	0.45%
Reinforcement	3 $\varnothing 8$	3 $\varnothing 6$	3 $\varnothing 8$
$f_{ccm,28d}$	58.8 MPa	58.1 MPa	57.5 MPa
$f_{ctm,28d}$	2.9 MPa	2.7 MPa	3.0-3.1 MPa
E_{cm}	32.5 GPa	30.5 GPa	31.0 GPa

2.2 Material

The concrete used for all the experiments was self-compacting (slump flow spread of 650 to 780 mm) and had a w/c-ratio between 0.53 and 0.55. Each batch contained 2 m³ concrete and was mixed

2.3 Pull-out tests

Bond properties between reinforcement bars and concrete are influenced by the fibre content. To study this phenomenon, pull-out tests were performed. To avoid wall effects the specimens were cut out from larger prisms of $110 \times 152 \times 720 \text{ mm}^3$; the specimen dimensions were $112 \times 112 \times 110 \text{ mm}^3$. A ribbed $\phi 16$ bar of quality B500BT was placed in the square cross-section centre. Specimen size was chosen so that the concrete surface strains would be measurable while delaying splitting in the series without steel fibre reinforcement as long as possible. Five specimens were tested for each fibre content. Full description of experiments and results is given in Jansson et al. [6].

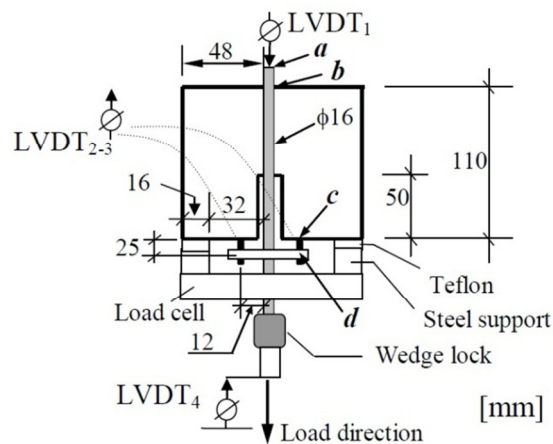


Figure 3: Geometry and test setup for pull-out testing [6].

3 NON-LINEAR FINITE ELEMENT ANALYSIS

Non-linear finite element analyses were performed using the commercial FE-software TNO DIANA [15]. A phased loading procedure was used. In the first phase, the selfweight was applied and incremental loading was applied by deformation control during the second phase. The model used is described in the following two sections.

3.1 Geometry

Concrete was represented by four-node quadrilateral isoperimetric plane stress elements. A dense quadratic mesh ($5 \times 5 \text{ mm}$) was used. The reinforcement was modeled by straight 2-point truss elements connected to two-dimensional interface elements providing the bondslip properties. Due to symmetry, half of a beam was modeled, see Figure 4. In the symmetry line, all movement in the horizontal direction was constrained. Both support and loading plates were modeled using eccentric tyings. In brief, the vertical movement of the nodes at the plates was maintained on a straight line intersecting the plate center node. Regions acting under these assumptions were 150 and 100 mm wide for the support node and the loading node, respectively. The support centre node was constrained from vertical movement.

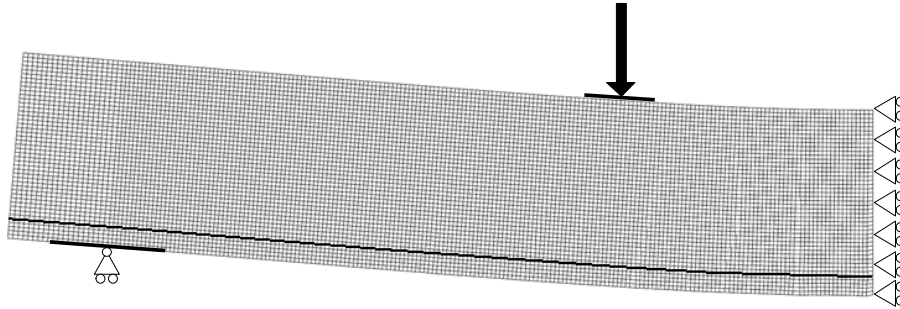


Figure 4: Model geometry. Eccentric boundary conditions (tyings) and the reinforcement position are indicated with thick black lines.

3.2 Material models

Nonlinear fracture mechanics with rotating cracks were used for concrete modeling. As previously mentioned, the tensile properties of the concrete were determined by uniaxial tension tests. The crackwidths, w_i , measured in these tests established the input for the tensile behavior of the concrete, see Figure 5. The smeared crack approach was utilized and the stress-strain relation given as input was calculated according to Equation 1, where the crack bandwidth, h , was assumed to be equal to the element length,

$$\varepsilon_i = \frac{f_t}{E} + \frac{w_i}{h}. \quad (1)$$

For compression, an elasto ideal-plastic compressive behavior formed the basis. However, in order to limit the effects of an oversimplistic compression model, a reduction function was used, taking into account the lower compressive stresses in elements with large tensile stress perpendicular to the principal compressive direction. The function is implemented in the software TNO DIANA [15] and is based on the theory of Vecchio and Collins [16]. Furthermore, the elastic modulus of the uncracked concrete was also established from the uniaxial tension tests and can be found in Table 1.

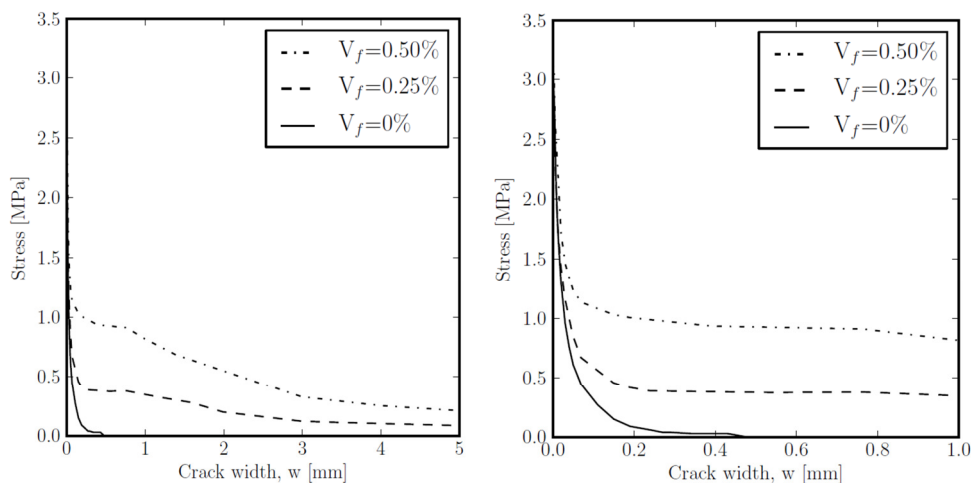


Figure 5: Input used for concrete tensile behaviour (left) and in detail for crack widths up to 1 mm (right).

A material model that included hardening effects was used for conventional reinforcement

bars. The material behavior was determined by five tension tests on each reinforcement type, as described in Section 2.2. In the model, the average nominal diameter of the reinforcement bars was used. The corresponding input is shown in Figure 6.

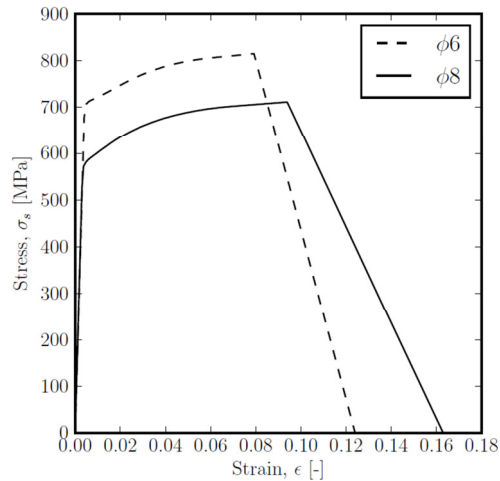


Figure 6: Input for the reinforcement bars

As described in Section 2-2, the bond-slip behavior was measured in the pull-out tests. Noteworthy is that the pull-out tests were performed on specimens with reinforcement bar diameter of 16 mm. However, as the ratio between the concrete cover thickness and the bar diameters is approximately the same in the pull-out specimens and beams, the bond stress versus slip measured in the pull-out tests was assumed to be directly applicable as input in the modeling of the beams.

As a reduction of bond stress after yielding of the reinforcement had been observed by numerous researchers, e.g. Shima et al. [17] and Engström [18], two analyses were carried out for all three beams: one in which the bond stress depended solely on the slip, and the other in which the bond stress was linearly reduced when yielding of the reinforcement occurred. In the latter case, the bond stress was linearly reduced when yielding occurred, see Figure 7. This model was suggested by Engström [18], who also verified that $\tau_{f,pl} = 0.5\tau_f$ and $s_4 = 0.5s_3$ are reasonable assumptions. These values were therefore applied in the current study, as shown in Figure 7b. The bond stress versus slip relations used as input are presented in Figure 7a. As shown a sudden and complete loss of bond in the specimens without fibres was observed in the pull-out tests. It can also be noted that contrary to what would be expected, the average bond capacity of the pull-out tests with $V_f = 0:50\%$ was lower than the average of the ones with less fibre content ($V_f = 0:25\%$). This is due to rather large scatter in the experimental results of the fibre content $V_f = 0:50\%$. In pull-out tests with higher fibre content ($V_f = 1:0\%$), presented in Jansson et al. [6], both the maximum and residual bond capacity increased.

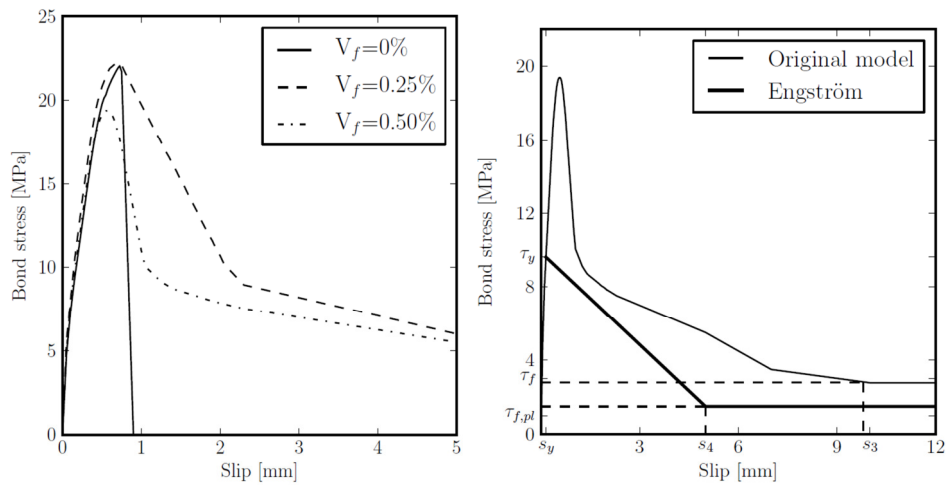


Figure 7: Bond stress versus slip used as input (left). Bond stress versus slip, original model and how it is modified when yielding occurs in reinforcement according to Engström [18], used for $V_f=0.50\%$ (right).

4 RESULTS

In this section focus is on the comparison between the performed beam tests, the FE-analyses and analyses according to MC2010. Load deflection curves, crack patterns and effect of bond reduction at yielding are presented and discussed separately. For a detailed description of the calculations in accordance with MC2010, see Fall et al. [19].

4.1 Load deflection

In Figure 8, results from experiments, analysis according to MC 2010 and FE-modeling can be seen. When comparing load deflection behavior, general agreement is shown. A first stiffness loss can be observed in all three beams when the first crack developed, followed by relatively constant stiffness until yielding of the reinforcement. All three beams failed in bending. Figure 8 shows that good agreement was obtained in the FE-analyses, both concerning ultimate load and deflection. Furthermore, it can be seen that in the analysis according to MC2010, both ultimate load and deflection were underestimated, and that this underestimation increased with increasing fibre content.

Considering the FE analysis of the beam without fibres, a sudden loss of stiffness was observed just after the yielding of the reinforcement (at a load of approximately 27kN), see Figure 8. It was observed that tensile strains developed locally in the elements surrounding the reinforcement bar, as a continuation of an inclined crack. The main direction of these cracks were along the bars; thus the crack pattern was similar to shear-splitting failure after this point.

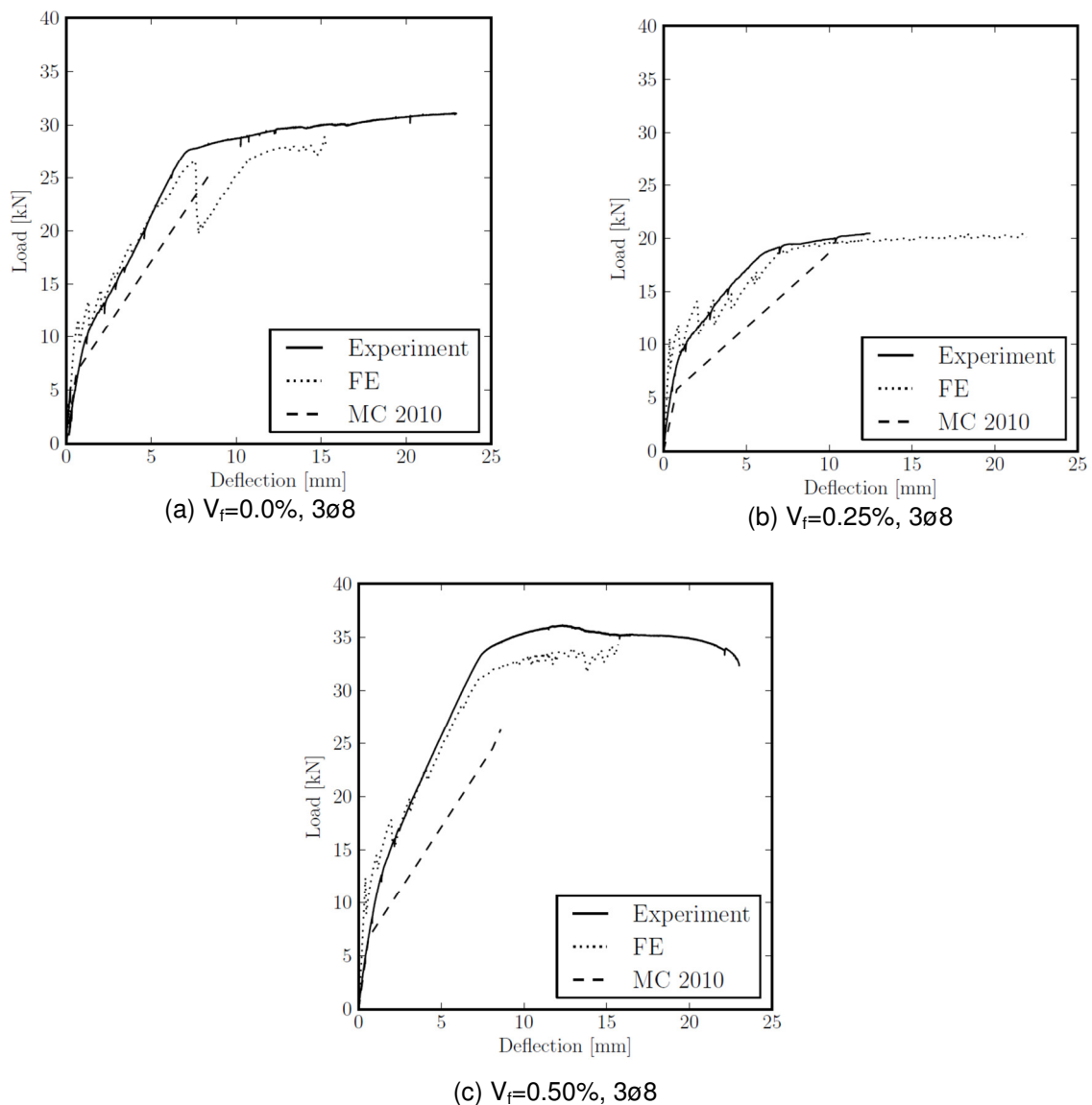


Figure 8: Load deflection behaviour (mid span): comparison between experiments, analysis according to MC 2010 and FE-modeling utilizing bond model according to Engström [18].

The FE analysis were stable and usually converged until some load steps after yielding occurred in the reinforcement. For larger deflections, the analyses did not converge in all steps; which can be seen in Figure 8 as small disturbances in the response. These disturbances are due to numerical problems.

4.2 Crack patterns

Crack patterns in experiments and from FE-analysis are compared in Figure 9. It can be seen that the number of cracks, the total spread and crack distance roughly agrees. In the tested beams the

position of the first crack depends on imperfections in e.g. sample and set-up, while in the FE-model the first crack always starts perfectly in midspan (due to the nature of the load combination with point-loads and self weight). This will naturally affect the positions of later cracks. In addition to this feature, the already mentioned imperfections in the experiments will further contribute to the somewhat varying crack positions. In Figure 9 half of the tested beams are displayed in order to facilitate the comparability. The omitted halves of the real beams had similar, but not exactly matching, patterns.

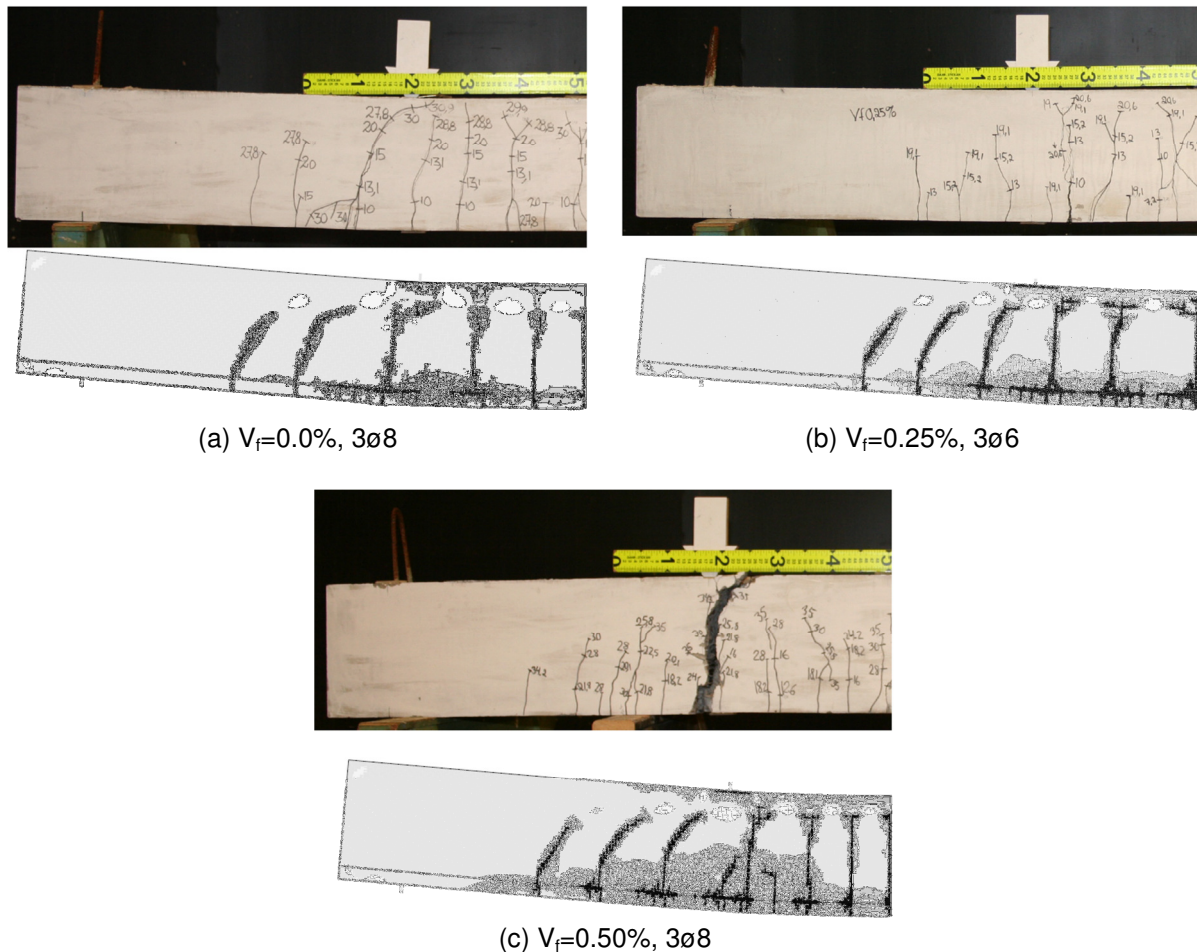


Figure 9: Crack patterns in experiments compared with those from FE analyses (using improved bond model). The applied deformation (in FE analyses) was 5.5 mm, 6.4 mm and 13.0 mm for $V_f=0\%$, $V_f=0.25\%$ and $V_f=0.50\%$ respectively

Furthermore, both in tests and in FE analyses the number of cracks tends to increase with the increasing fibre content. This relation was expected since it has been previously observed [7, 20, 21]. From the FE-analyses the crack spacing can be estimated by measuring the distance between the cracks in a contour plot of the maximum tensile strain. The measured crack spacing is then averaged and compared to the calculated crack spacing according to MC 2010. In Table 5 the measured crack spacing from experiments and FE-analyses is presented together with the calculated. It can be noted that the crack spacing in the finite element analysis are overestimated, ranging from very minor to rather large overestimation. Furthermore, there is no clear trend regarding the crack spacing

calculated according to MC2010: it is overestimated for the beam with $V_f = 0:25\%$, but is underestimated for the beam with $V_f = 0:50\%$. To be able to draw clear conclusions, more cases need to be studied.

Table 2: Measured crack spacing from experiments, $l_{s,mean,exp}$, and finite element analyses, $l_{s,mean,fe}$, compared with calculated values of crack spacing according to MC 2010, $l_{s,mean,MC2010}$, for the studied beams.

Beam	Measured $l_{s,mean,exp}$ [mm]	Modeled $l_{s,mean,FE}$ [mm]	Calculated $l_{s,mean,MC2010}$ [mm]
$V_f=0.0\%$, 3 \emptyset 8	69	90	69
$V_f=0.25\%$, 3 \emptyset 6	70	139	92
$V_f=0.50\%$, 3 \emptyset 8	61	64	53

4.3 Effect of bond reduction at yielding

As previously described in Section 3-2, two analyses of each beam were carried out: one with original bond-slip model and one where the bond stress was linearly decreased with increased slip once yielding occurred in the reinforcement bar [18]. There was no difference in cracking before yielding of the reinforcement, as the two bond models were completely equivalent up until this point, see Figure 10. As expected the cracks were more clearly localized when the bond stress is reduced at yielding. This is due to the fact that when the bond stress does not increase after yielding of the reinforcement, no new cracks form.

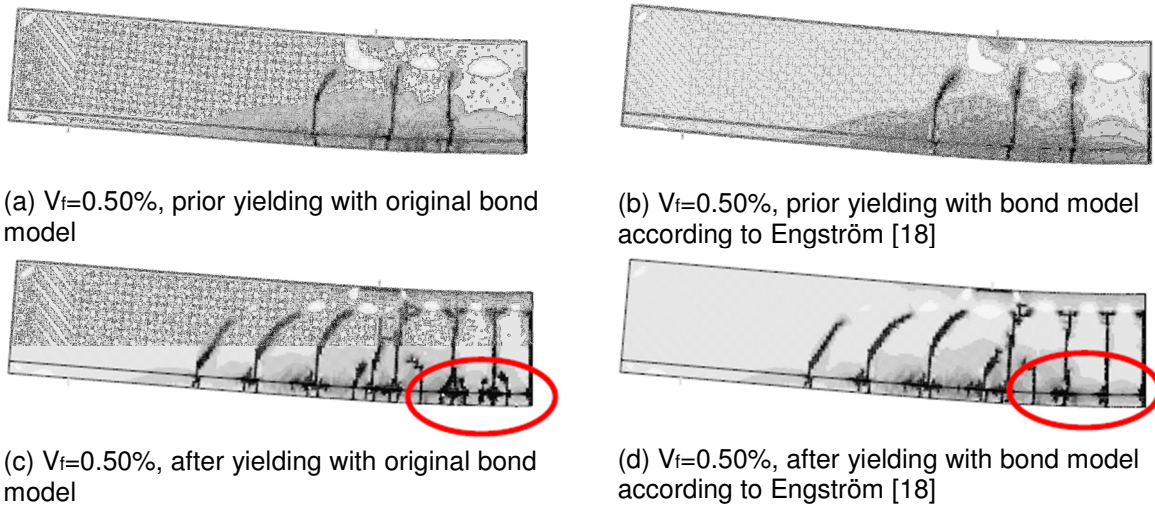


Figure 10: Examples of crack patterns, $V_f=0.50\%$, corresponding to the applied deformation 2.7 mm (a and b) and 14 mm (c and d). The distinct difference in crack localization after yielding of the reinforcement occurred is indicated.

5 CONCLUSIONS

Based on the work presented in this paper the following conclusions can be drawn:

1. The increased post cracking capacity of SFRC, seen in experiments, can be estimated with FE-analysis. However, MC 2010 fails to fully quantify such effects.

2. Reasonable agreement was also obtained with regards to crack patterns when comparing experiments and FE-analyses. Compared with MC 2010, the crack spacing obtained from finite element analyses were larger in all three beams.
3. Utilizing a bond-stress model where the bond stress is reduced post yielding, resulted in more localized crack patterns.
4. Modeling fibre reinforced concrete with non-linear finite element method, utilizing a 2D-model with plane stress elements were shown to be successful provided that material data is chosen with care. The calculation process is though characterized by long calculation time and convergence problems.
5. The method for analysis presented in MC2010 underestimates the additional capacity provided by the addition of steel fibres, in this specific type of beam, both with regards to load and deformation capacities. The underestimation increases with increased fibre content.
6. The calculation method proposed in MC2010 is hard to interpret. Fibre reinforcement needs to be included in all sections of fib Model Code in future versions.

ACKNOWLEDGEMENTS

The presented experiments were financed by Thomas Concrete Group AB. All other parts of this research were funded from the European Community's Seventh Framework Programme under grant agreement NMP2-LA-2009-228663 (TailorCrete). More information on the research project TailorCrete can be found at www.tailorcrete.com.

REFERENCES

- [1] A.G. Kooiman, C. Van Der Veen and J.C. Walraven, "Modelling the post-cracking behaviour of steel fibre reinforced concrete for structural design purposes", *Heron*, 45(4), 275-307 (2000).
- [2] G. Giaccio, J.M. Tobes and R. Zerbino, "Use of small beams to obtain design parameters of fibre reinforced concrete", *Cement and Concrete Composites*, 30(4), 297-306 (2008).
- [3] I. Löfgren, H. Stang and J.F. Olesen, "Fracture properties of FRC determined through inverse analysis of wedge splitting and three-point bending tests", *Journal of Advanced Concrete Technology*, 3(3), 423-434 (2005).
- [4] K. Noghabai, "Beams of Fibrous Concrete in Shear and Bending: Experiment and Model", *Journal of Structural Engineering*, 126(2), 243-251 (2000).
- [5] A. Jansson, I. Löfgren and K. Gylltoft, "Flexural Behaviour of Members with a Combination of Steel Fibres and Conventional Reinforcement", *Nordic Concrete Research*, 42), 155-171 (2010).
- [6] A. Jansson, I. Löfgren, K. Lundgren and K. Gylltoft, "Bond of Reinforcement in Self-Compacting Steel-Fibre Reinforced Concrete", *Provisionally accepted for publication in Magazine of Concrete Research*, (2011).
- [7] A. Jansson, M. Flansbjer, I. Löfgren and K. Gylltoft, "Experimental Investigation of Surface Crack Initiation, Propagation and Tension Stiffening in Self-Compacting Steel-Fibre Reinforced concrete", *Submitted to Materials and Structures*, (2011).
- [8] A. Jansson, Fibres in reinforced concrete structures, Licentiate Thesis, Department of Civil Engineering, Chalmers University of Technology, (2008).
- [9] M. Gustafsson and H. Karlsson, Fibre-reinforced concrete structures - Analysis of crack spacing and crack width (In Swedish: Fiberarmerade betongkonstruktioner - Analys av sprickavstånd och sprickbredd), M.Sc, Dep. of Structural Engineering Chalmers University of Technology, (2006).
- [10] SIS, SS-EN 14721:2005 Test method for metallic fibre concrete - Measuring the fibre content in fresh and hardened concrete, Swedish Standards Institute (SIS) (2005).
- [11] SIS, SS-EN 12390-3:2009 Testing hardened concrete - Part 3: Compressive strength of test specimens, Swedish Standards Institute (SIS) (2009).

- [12] SIS, SS-EN 137232:2005 Concrete testing - Hardened concrete - Modulus of elasticity in compression, Swedish Standards Institute (SIS) (2005).
- [13] SIS, SS-EN 12390-6:2009 Testing hardened concrete - Part 6: Tensile splitting strength of test specimens, Swedish Standards Institute (SIS) (2009).
- [14] RILEM TC 162-TDF, "Uni-axial tension test for steel fibre reinforced concrete", *Materials and Structures*, 34(1), 3-6 (2001).
- [15] T. DIANA, Finite element analysis, Users Manual Release 9.4.3, TNO (2010).
- [16] F.J. Vecchio and M.P. Collins, "Compression Response of Cracked Reinforced Concrete", *Journal of Structural Engineering*, 119(12), 3590-3610 (1993).
- [17] H. Shima, L. Chou and H. Okamura, "Bond Characteristics in Post-Yield Range of Deformed Bars", *Concrete Library International*, 10), 113-124 (1987).
- [18] B. Engström, Ductility of Tie Connections in Precast Structures, Ph.D. Thesis, Department of Civil Engineering, Chalmers University of Technology, (1992).
- [19] D. Fall, R. Rempling, A. Jansson, K. Lundgren and K. Gylltoft, "Steel fibres in reinforced beams: Experiments, model code and FE-analyses", *Submitted to Journal of Advanced Concrete Technology*, (2011).
- [20] J.S. Lawler, D. Zampini and S.P. Shah, "Microfiber and Macrofiber Hybrid Fiber-Reinforced Concrete", *Journal of Materials in Civil Engineering*, 7(5), 595-604 (2005).
- [21] P.H. Bischoff, "Tension Stiffening and Cracking of Steel Fiber-Reinforced Concrete", *Journal of Materials in Civil Engineering*, 15(2), 174-185 (2003).